SCIENCE CHINA
Mathematics

Progress of Projects Supported by NSFC
• ARTICLES •

June 2018 Vol. 61 No. 6: 973–992
https://doi.org/10.1007/s11425-017-9181-2

Residual-based a posteriori error estimates for symmetric conforming mixed finite elements for linear elasticity problems

Long Chen[1], Jun Hu[2], Xuehai Huang[3] & Hongying Man[4,*]

[1]*Department of Mathematics, University of California at Irvine, Irvine, CA* 92697*, USA;*
[2]*LMAM and School of Mathematical Sciences, Peking University, Beijing* 100871*, China;*
[3]*College of Mathematics and Information Science, Wenzhou University, Wenzhou* 325035*, China;*
[4]*School of Mathematics and Statistics, Beijing Institute of Technology, Beijing* 100081*, China*

Email: chenlong@math.uci.edu, hujun@math.pku.edu.cn, xuehaihuang@gmail.com, manhy@bit.edu.cn

Received June 2, 2017; accepted October 30, 2017; published online March 13, 2018

Abstract A posteriori error estimators for the symmetric mixed finite element methods for linear elasticity problems with Dirichlet and mixed boundary conditions are proposed. Reliability and efficiency of the estimators are proved. Numerical examples are presented to verify the theoretical results.

Keywords symmetric mixed finite element, linear elasticity problems, a posteriori error estimator, adaptive method

MSC(2010) 65N30, 73C02

Citation: Chen L, Hu J, Huang X H, et al. Residual-based a posteriori error estimates for symmetric conforming mixed finite elements for linear elasticity problems. Sci China Math, 2018, 61: 973–992, https://doi.org/10.1007/s11425-017-9181-2

1 Introduction

In this paper, we are concerned with the development of residual-based *a posteriori* error estimators for the symmetric mixed finite element methods for planar linear elasticity problems. Let $\Omega \subset \mathbb{R}^2$ be a bounded polygonal domain with boundary $\Gamma := \partial\Omega$, based on the Hellinger-Reissner principle, the linear elasticity problem with homogeneous Dirichlet boundary condition within a stress-displacement form reads: find $(\sigma, u) \in \Sigma \times V := H(\mathrm{div}, \Omega; \mathbb{S}) \times L^2(\Omega; \mathbb{R}^2)$, such that

$$\begin{cases} (A\sigma, \tau) + (\mathrm{div}\tau, u) = 0 & \text{for all} \quad \tau \in \Sigma, \\ (\mathrm{div}\sigma, v) = (f, v) & \text{for all} \quad v \in V, \end{cases} \tag{1.1}$$

where $\mathbb{S} \subset \mathbb{R}^{2\times 2}$ is the space of symmetric matrices, and the symmetric tensor space for stress and the space for vector displacement are, respectively,

$$H(\mathrm{div}, \Omega; \mathbb{S}) := \{(\tau_{ij})_{2\times 2} \in H(\mathrm{div}, \Omega) \,|\, \tau_{12} = \tau_{21}\}, \tag{1.2}$$

$$L^2(\Omega; \mathbb{R}^2) := \{(u_1, u_2)^{\mathrm{T}} \,|\, u_1, u_2 \in L^2(\Omega)\}. \tag{1.3}$$

* Corresponding author

The compliance tensor $A:\mathbb{S}\rightarrow\mathbb{S}$, characterizing the properties of the material, is symmetric positive definite and its eigenvalues are uniformly bounded from above. In the homogeneous isotropic case, the compliance tensor is given by $A\tau=(\tau-\lambda/(2\mu+2\lambda)\mathrm{tr}\tau\mathrm{I})/(2\mu)$, where $\mu>0$ and $\lambda\geqslant 0$ are the Lamé constants, I is the identity matrix, and $\mathrm{tr}\tau=\tau_{11}+\tau_{22}$ is the trace of the matrix τ. For simplicity, we assume A is a constant matrix in this paper and comment on the generalization to the piecewise constant matrix case.

Because of the symmetry constraint on the stress tensor, it is extremely difficult to construct stable conforming finite elements of (1.1) even for 2D problems, as stated in the plenary presentation to the 2002 International Congress of Mathematicians by Arnold [3]. To overcome this difficulty, many weakly symmetric mixed finite element methods for linear elasticity were developed (see [6, 7, 10, 21, 25]). An important progress in this direction is the work of Arnold and Winther [8] and Arnold et al. [5]. In particular, a sufficient condition of the discrete stable method is proposed in these two papers, which states that a discrete exact sequence guarantees the stability of the mixed method. Based on such a condition, conforming mixed finite elements on the simplical and rectangular meshes were developed for both 2D and 3D (see [1, 4, 5, 8, 9]). Recently, based on a crucial structure of symmetric matrix valued piecewise polynomial $H(\mathrm{div})$ space and two basic algebraic results, Hu [27,28] developed a new framework to design and analyze the mixed finite element of elasticity problems. As a result, on both simplicial and tensor product grids, several families of both symmetric and optimal mixed elements with polynomial shape functions in any space dimension were constructed (see more details in [27–31]). Theoretical and numerical analysis show that symmetric mixed finite element method is a popular choice for a robust stress approximation (see [15, 17]).

Computation with adaptive grid refinement has been proved to be a useful and efficient tool in scientific computing over the last several decades. When the domain contains a re-entering corner, the stress has a singularity at that corner, and non-uniform mesh is necessary to catch the singularity. Adaptive finite element methods based on local mesh refinement can recover the optimal rate of convergence. The key behind this technique is to design a good *a posteriori* error estimator that provides a guidance on how and where grids should be refined. The residual-based *a posteriori* error estimators provide indicators for refining and coarsening the mesh and allow to control whether the error is below a given threshold. Various error estimators for mixed finite element discretizations of the Poisson equation have been obtained in [2, 13, 19, 22, 26, 33, 35]. Extension to the mixed finite element for linear elasticity is, however, very limited. In [14, 32, 34], the authors gave the *a posteriori* error estimators for the nonsymmetric mixed finite elements only.

The symmetry of the stress tensor brings essential difficulty to the *a posteriori* error analysis. Since only the symmetric part is approximated and not the full gradient, the approach of *a posteriori* error analysis developed in [14, 18, 32, 34] cannot be applied directly. In order to overcome this difficulty, Carstensen and Gedicke [16] proposed to generalize the framework of the *a posteriori* analysis for nonsymmetric mixed finite elements to the case of symmetric elements by decomposing the stress into the gradient and the asymmetric part of the gradient. A robust residual-based *a posteriori* error estimator for Arnold-Winther's symmetric element was proposed in [16], but an arbitrary asymmetric approximation γ_h of the asymmetric part of the gradient $\mathrm{skew}(\mathrm{grad}u)=(\mathrm{grad}u-(\mathrm{grad}u)^{\mathrm{T}})/2$ was involved in this estimator. Furthermore, γ_h was chosen as the asymmetric gradient of a post-processed displacement to ensure the efficiency of the estimator.

The goal of this paper is to present an *a posteriori* error estimator together with a theoretical upper and lower bounds, for the conforming and symmetric mixed finite element solutions developed in [8, 29] (see also [27, 31]). We shall follow the guide principle in [8]: use the continuous and discrete linear elasticity complex (see (2.2) and (2.3)).

Given an approximation σ_h on the triangulation $\mathcal{T}_h$ consisting of triangles, we construct the following *a posteriori* error estimator: denoted by η,

$$\eta^2(\sigma_h,\mathcal{T}_h):=\sum_{K\in\mathcal{T}_h}\eta_K^2(\sigma_h)+\sum_{e\in\mathcal{E}_h}\eta_e^2(\sigma_h),$$

where

$$\eta_K^2(\sigma_h) := h_K^4\|\mathrm{curl}\,\mathrm{curl}\,(A\sigma_h)\|_{0,K}^2, \quad \eta_e^2(\sigma_h) := h_e\|\mathcal{J}_{e,1}\|_{0,e}^2 + h_e^3\|\mathcal{J}_{e,2}\|_{0,e}^2,$$

$$\mathcal{J}_{e,1} := \begin{cases} [(A\sigma_h)t_e \cdot t_e]_e, & \text{if } e \in \mathcal{E}_h(\Omega), \\ ((A\sigma_h)t_e \cdot t_e)\,|_e, & \text{if } e \in \mathcal{E}_h(\Gamma), \end{cases}$$

$$\mathcal{J}_{e,2} := \begin{cases} [\mathrm{curl}(A\sigma_h) \cdot t_e]_e, & \text{if } e \in \mathcal{E}_h(\Omega), \\ (\mathrm{curl}(A\sigma_h) \cdot t_e - \partial_{t_e}((A\sigma_h)t_e \cdot \nu_e))\,|_e, & \text{if } e \in \mathcal{E}_h(\Gamma), \end{cases}$$

with $\mathcal{E}_h$ being the collection of all edges of $\mathcal{T}_h$. We write $\mathcal{E}_h = \mathcal{E}_h(\Omega) \cup \mathcal{E}_h(\Gamma)$, where $\mathcal{E}_h(\Omega)$ is the collection of interior edges and $\mathcal{E}_h(\Gamma)$ is the collection of all element edges on the boundary. For any edge $e \in \mathcal{E}_h$, let $t_e = (-n_2, n_1)^{\mathrm{T}}$ be the unit tangential vector along edge e for the unit outward normal $\nu_e = (n_1, n_2)^{\mathrm{T}}$. Let h_K be the diameter of the element K and h_e be the length of edge e. The data oscillation is defined as

$$\mathrm{osc}^2(f, \mathcal{T}_h) := \sum_{K \in \mathcal{T}_h} h_K^2 \|f - Q_h f\|_{0,K}^2,$$

where Q_h is the L^2 orthogonal projection operator onto the discrete displacement space.

Using the Helmholtz decomposition induced from the linear elasticity complex (see [8,14]), we establish the following reliability:

$$\|\sigma - \sigma_h\|_A \leqslant C_1(\eta(\sigma_h, \mathcal{T}_h) + \mathrm{osc}(f, \mathcal{T}_h)).$$

In addition, we will prove the following efficiency estimate:

$$C_2\eta(\sigma_h, \mathcal{T}_h) \leqslant \|\sigma - \sigma_h\|_A$$

by following the approach from [2].

We also generalize the above results to the mixed boundary problems, for which the error estimator is modified on the Dirichlet boundary edges. Reliability and efficiency of the modified error estimator can be proved similarly.

In [20], a superconvergent approximate displacement u_h^* was constructed by a postprocessing of (σ_h, u_h). Using this result and the *a posteriori* error estimation of the stress, we give the *a posteriori* error estimation for the displacement $\|u - u_h^*\|_{1,h}$ in a mesh dependent norm.

In order to compare with the *a posteriori* error estimator in [16], we present their estimator as follows:

$$\begin{aligned} \tilde{\eta}^2(\sigma_h, \mathcal{T}_h) := {} & \mathrm{osc}^2(f, \mathcal{T}_h) + \mathrm{osc}^2(g, \mathcal{E}_h(\Gamma_N)) \\ & + \sum_{K \in \mathcal{T}} h_K^2 \|\mathrm{curl}(A\sigma_h + \gamma_h)\|_{0,K}^2 \\ & + \sum_{e \in \mathcal{E}_h(\Omega)} h_e \|[A\sigma_h + \gamma_h]_e \tau_e\|_{0,e}^2 \\ & + \sum_{e \in \mathcal{E}_h(\Gamma_D)} h_e \|(A\sigma_h + \gamma_h - \nabla u_D)\tau_e\|_{0,e}^2. \end{aligned}$$

(The estimator is rewritten in our notation and the details of the standard notation can be found below.) To ensure the efficiency of the estimator, a sufficiently accurate polynomial asymmetric approximation γ_h of the asymmetric gradient skew(grad$u$) is used in the above estimator. Since the global approximation or even minimization may be too costly, Carstensen and Gedicke [16] computed the sufficiently accurate approximation $\gamma_h = \mathrm{skew}(\mathrm{grad} u_h^*)$ by the post-processed displacement u_h^* in the spirit of Stenberg [38]. As we can see, this estimator is totally different from ours. The estimators we propose use the symmetric stress directly and do not need any estimation of the asymmetric part. Therefore it is more computationally efficient.

The remaining parts of the paper is organized as follows. Section 2 presents the notation and the discrete finite element problems. Section 3 proposes an *a posteriori* error estimator for the stress and proves the reliability and efficiency of the estimator. Section 4 generalizes the results of Section 3 to mixed boundary problems. Section 5 gives *a posteriori* error estimation for the displacement. Section 6 presents numerical experiments to show the effectiveness of the estimator. Throughout this paper, we use "$\lesssim \cdots$" to mean that "$\leqslant C\cdots$", where C is a generic positive constant independent of h and the Lamé constant λ, which may take different values at different appearances.

2 Notation and preliminaries

The standard notation on Sobolev spaces and norms are adopted throughout this paper and, for brevity, $\|\cdot\| := \|\cdot\|_{L^2(\Omega)}$ denotes the L^2 norm. $(\cdot,\cdot)_K$ represents, as usual, the L^2 inner product on the domain K, the subscript K is omitted when $K=\Omega$. $\langle\cdot,\cdot\rangle_\Gamma$ represents the L^2 inner product on the boundary Γ. For brevity, let $\partial_{x_i} := \partial/\partial x_i$ and $\partial^2_{x_ix_j} := \partial^2/\partial x_i\partial x_j, j=1,2$, $\partial_\nu := \partial/\partial\nu$, $\partial_t := \partial/\partial t$. For $\phi\in H^1(\Omega;\mathbb{R})$, $v=(v_1,v_2)^{\mathrm{T}}\in H^1(\Omega;\mathbb{R}^2)$, set

$$\mathbf{Curl}\phi := (-\partial\phi/\partial x_2, \partial\phi/\partial x_1), \quad \mathbf{Curl}v := \begin{pmatrix} -\partial v_1/\partial x_2 & \partial v_1/\partial x_1 \\ -\partial v_2/\partial x_2 & \partial v_2/\partial x_1 \end{pmatrix}.$$

The symmetric part of the gradient of a vector field v, denoted by $\varepsilon(v)$, is given by

$$\varepsilon(v) := (\mathrm{grad}v + (\mathrm{grad}v)^{\mathrm{T}})/2.$$

For $\tau=(\tau_{i,j})_{2\times 2}\in H^1(\Omega;\mathbb{R}^{2\times 2})$, set

$$\mathrm{curl}\tau := \begin{pmatrix} \partial\tau_{12}/\partial x_1 - \partial\tau_{11}/\partial x_2 \\ \partial\tau_{22}/\partial x_1 - \partial\tau_{21}/\partial x_2 \end{pmatrix}, \quad \mathrm{div}\tau := \begin{pmatrix} \partial\tau_{11}/\partial x_1 + \partial\tau_{12}/\partial x_2 \\ \partial\tau_{21}/\partial x_1 + \partial\tau_{22}/\partial x_2 \end{pmatrix}.$$

Namely the differential operators curl and div are applied rowwise for tensors.

Let $\mathcal{T}_h$ be a shape-regular triangulation of $\bar\Omega$ into triangles with the set of edges $\mathcal{E}_h$. Denote by $\mathcal{E}_h(\Omega)$ the collection of all interior element edges in $\mathcal{T}_h$ and $\mathcal{E}_h(\Gamma)$ the collection of all element edges on the boundary Γ. For any triangle $K\in\mathcal{T}_h$, let $\mathcal{E}(K)$ be the set of its edges. For any edge $e\in\mathcal{E}(K)$, let $t_e=(-n_2,n_1)^{\mathrm{T}}$ be the unit tangential vector along edge e for the unit outward normal vector $\nu_e=(n_1,n_2)^{\mathrm{T}}$, h_K be the diameter of the element K and h_e be the length of the edge e, $h=\max_{K\in\mathcal{T}_h}\{h_K\}$ be the diameter of the partition $\mathcal{T}_h$. The jump $[w]_e$ of w across edge $e=\bar K_+\cap\bar K_-$ reads

$$[w]_e := (w\,|_{K_+})_e - (w\,|_{K_-})_e.$$

Particularly, if $e\in\mathcal{E}_h(\Gamma)$, $[w]_e := w\,|_e$.

Let $\Sigma_h\times V_h\subseteq\Sigma\times V$ be a symmetric conforming mixed element defined on the mesh $\mathcal{T}_h$. Then the discrete mixed formulation for (1.1) is: find $(\sigma_h,u_h)\in\Sigma_h\times V_h$, such that

$$\begin{cases} (A\sigma_h,\tau_h)+(\mathrm{div}\tau_h,u_h)=0 & \text{for all } \tau_h\in\Sigma_h, \\ (\mathrm{div}\sigma_h,v_h)=(f,v_h) & \text{for all } v_h\in V_h. \end{cases} \tag{2.1}$$

In the sequel, we briefly introduce Hu-Zhang element (see [27,29,31]). For each $K\in\mathcal{T}_h$, let $P_k(K)$ be the space of polynomials of total degree at most k on K and

$$P_k(K;\mathbb{S}) := \{\tau\in L^2(K;\mathbb{R}^{2\times 2})\,|\tau_{i,j}\in P_k(K), \tau_{ij}=\tau_{ji}, 1\leqslant i\leqslant 2, 1\leqslant j\leqslant 2\},$$
$$P_k(K;\mathbb{R}^2) := \{v\in L^2(K;\mathbb{R}^2)\,|v_i\in P_k(K), 1\leqslant i\leqslant 2\},$$

define an $H(\mathrm{div},K;\mathbb{S})$ bubble function as

$$B_{K,k} := \{\tau\in P_k(K;\mathbb{S}) : \tau\nu\,|_{\partial K}=0\}.$$

The Hu-Zhang element space is given by

$$\Sigma_h := \widetilde\Sigma_{k,h} + B_{k,h},$$

$$V_h := \{v \in L^2(\Omega;\mathbb{R}^2) : v\,|_K \in P_{k-1}(K;\mathbb{R}^2), \forall\, K \in \mathcal{T}_h\},$$

with integer $k \geqslant 3$, where

$$B_{k,h} := \{\tau \in H(\mathrm{div},\Omega;\mathbb{S}) : \tau\,|_K \in B_{K,k}, \forall\, K \in \mathcal{T}_h\},$$
$$\widetilde{\Sigma}_{k,h} := \{\tau \in H^1(\Omega;\mathbb{S}) : \tau\,|_K \in P_k(K;\mathbb{S}), \forall\, K \in \mathcal{T}_h\}.$$

For the above elements, the following *a priori* error estimate holds.

Theorem 2.1 (A priori error estimate, see [27, 29, 31]). *The exact solution* (σ, u) *of* (1.1) *and the approximate solution* (σ_h, u_h) *of* (2.1) *satisfy*

$$\|\sigma-\sigma_h\|_0 \lesssim h^m\|\sigma\|_m, \quad \text{for } 1 \leqslant m \leqslant k+1,$$
$$\|\mathrm{div}(\sigma-\sigma_h)\|_0 \lesssim h^m\|\mathrm{div}\sigma\|_m, \quad \text{for } 0 \leqslant m \leqslant k,$$
$$\|u-u_h\|_0 \lesssim h^m\|u\|_{m+1}, \quad \text{for } 1 \leqslant m \leqslant k.$$

In the continuous case, the following exact sequence:

$$P_1(\Omega) \longrightarrow H^2(\Omega) \stackrel{\mathbf{CurlCurl}}{\longrightarrow} H(\mathrm{div},\Omega;\mathbb{S}) \stackrel{\mathrm{div}}{\longrightarrow} L^2(\Omega,\mathbb{R}^2) \tag{2.2}$$

holds for linear elasticity (see [8]). In the discrete case, the exact sequence holds similarly

$$P_1(\Omega) \longrightarrow \Phi_h \stackrel{\mathbf{CurlCurl}}{\longrightarrow} \Sigma_h \stackrel{\mathrm{div}}{\longrightarrow} V_h. \tag{2.3}$$

As stated in [8], the space Φ_h for the Arnold-Winther element is precisely the space of C^1 piecewise polynomials which are C^2 at the vertices, i.e., the well-known high-order Hermite or Argyris finite element. The Hu-Zhang element is an enrichment of the Arnold-Winther element, adding all the piecewise polynomial matrices of degree k which are not divergence-free on each element and belong to $H(\mathrm{div},\Omega;\mathbb{S})$ globally. So the space Φ_h for the Hu-Zhang element is the same as the one for the Arnold-Winther element.

Lemma 2.2 (Helmholtz-type decomposition, see [8, 14]). *For any* $\tau \in L^2(\Omega;\mathbb{S})$, *there exist* $v \in H_0^1(\Omega;\mathbb{R}^2)$ *and* $\phi \in H^2(\Omega)/P_1(\Omega)$, *such that*

$$\tau = \mathcal{C}\varepsilon(v) + \mathbf{CurlCurl}\phi, \tag{2.4}$$

and the decomposition is orthogonal in the weighted L^2*-inner product* $(\mathcal{C}^{-1}\cdot,\cdot) := (A\ \cdot,\cdot)$, *i.e.,*

$$\|\tau\|_A^2 = \|\varepsilon(v)\|_{A^{-1}}^2 + \|\mathbf{CurlCurl}\phi\|_A^2, \tag{2.5}$$

where $P_1(\Omega)$ *is the linear polynomial space on* Ω, *the norm* $\|\cdot\|_A^2 = (A\ \cdot,\cdot)$.

Since

$$(A^{-1}A\tau,\tau) = (\tau,\tau) = (A(A^{-1}\tau),\tau),$$

by the boundedness and coerciveness of the operator A, we obtain the following relationship of the norms: for any $\tau \in \Sigma$, there exist positive constants C_1 and C_2, which are independent of the Lamé constant λ, such that

$$C_2\|\tau\|_A^2 = C_2(A\tau,\tau) \leqslant \|\tau\|_0^2 \leqslant C_1(A^{-1}\tau,\tau) = C_1\|\tau\|_{A^{-1}}^2. \tag{2.6}$$

It is the goal of this paper to present *a posterior* error estimate of $\sigma-\sigma_h$ for the Hu-Zhang element method. It is worth mentioning that the *a posterior* error estimator designed in this paper can be easily extended to the Arnold-Winther element (see [8]).

3 A posteriori error estimation for stress

In this section, we shall prove the reliability and efficiency of the error estimator. The main observation is that: although it is a saddle point problem, the error of stress $\sigma - \sigma_h$ is orthogonal to the divergence-free subspace, while the part of the error that is not divergence-free can be bounded by the data oscillation using the stability of the discretization.

For any $\tau_h \in \Sigma_h$, the error estimator is defined as

$$\eta^2(\tau_h, \mathcal{T}_h) := \sum_{K \in \mathcal{T}_h} \eta_K^2(\tau_h) + \sum_{e \in \mathcal{E}_h} \eta_e^2(\tau_h), \tag{3.1}$$

where

$$\eta_K^2(\tau_h) := h_K^4 \|\mathrm{curl}\,\mathrm{curl}\,(A\tau_h)\|_{0,K}^2, \quad \eta_e^2(\tau_h) := h_e \|\mathcal{J}_{e,1}\|_{0,e}^2 + h_e^3 \|\mathcal{J}_{e,2}\|_{0,e}^2,$$
$$\mathcal{J}_{e,1} := \begin{cases} [(A\tau_h)t_e \cdot t_e]_e, & \text{if } e \in \mathcal{E}_h(\Omega), \\ ((A\tau_h)t_e \cdot t_e)\,|_e, & \text{if } e \in \mathcal{E}_h(\Gamma), \end{cases}$$
$$\mathcal{J}_{e,2} := \begin{cases} [\mathrm{curl}(A\tau_h) \cdot t_e]_e, & \text{if } e \in \mathcal{E}_h(\Omega), \\ (\mathrm{curl}(A\tau_h) \cdot t_e - \partial_{t_e}((A\tau_h)t_e \cdot \nu_e))\,|_e, & \text{if } e \in \mathcal{E}_h(\Gamma). \end{cases}$$

The data oscillation is defined as

$$\mathrm{osc}^2(f, \mathcal{T}_h) := \sum_{K \in \mathcal{T}_h} h_K^2 \|f - Q_h f\|_{0,K}^2,$$

where Q_h is the L^2 orthogonal projection operator onto the discrete displacement space V_h.

3.1 Stability result

For the ease of exposition, we write the mixed formulation for linear elasticity as $\mathcal{L}(\sigma, u) = f$. The natural stability of the operator is $\|\sigma\|_{H(\mathrm{div})} + \|u\| \lesssim \|f\|$. However, a stronger stability can be proved for a special perturbation of the data.

Lemma 3.1. *Let f_h be the L^2 projection of f onto V_h and let $(\sigma, u) = \mathcal{L}^{-1} f$ and $(\tilde{\sigma}, \tilde{u}) = \mathcal{L}^{-1} f_h$. Then we have*

$$\|\sigma - \tilde{\sigma}\|_A \lesssim \mathrm{osc}(f, \mathcal{T}_h). \tag{3.2}$$

Proof. Use the first equation of (1.1) and let $v = u - \tilde{u}$,

$$\begin{aligned} (A(\sigma - \tilde{\sigma}), \sigma - \tilde{\sigma}) &= -(\mathrm{div}(\sigma - \tilde{\sigma}), u - \tilde{u}) = -(f - Q_h f, u - \tilde{u}) \\ &= (f - Q_h f, Q_h v - v) \\ &\leqslant \sum_{K \in \mathcal{T}_h} \|f - Q_h f\|_{0,K} \|v - Q_h v\|_{0,K} \\ &\lesssim \sum_{K \in \mathcal{T}_h} \|f - Q_h f\|_{0,K} h_K |v|_{1,K} \\ &\lesssim \Bigg(\sum_{K \in \mathcal{T}_h} h_K^2 \|f - Q_h f\|_{0,K}^2 \Bigg)^{\frac{1}{2}} \|\varepsilon(v)\|_0, \end{aligned}$$

where the Korn's inequality is used. Since $\varepsilon(v) = A(\sigma - \tilde{\sigma})$, by (2.6),

$$\|\varepsilon(v)\|_0 \lesssim \|\sigma - \tilde{\sigma}\|_A.$$

We acquire the desirable stability result. □

The oscillation $\mathrm{osc}(f, \mathcal{T}_h)$ is an upper bound of $\|f - f_h\|_{-1}$ and is of high order comparing with the error estimator.

3.2 Orthogonality

For any $\phi \in H^2(\Omega)$, $\mathbf{CurlCurl}\phi \in H(\mathrm{div}, \Omega; \mathbb{S})$, we can use the exact sequence property $\mathrm{div}\, \mathbf{CurlCurl} = 0$ to get

$$(A\tilde{\sigma}, \mathbf{CurlCurl}\phi) = -(\tilde{u}, \mathrm{div}\, \mathbf{CurlCurl}\phi) = 0. \tag{3.3}$$

Similarly

$$(A\sigma_h, \mathbf{CurlCurl}\phi_h) = -(u_h, \mathrm{div}\, \mathbf{CurlCurl}\phi_h) = 0$$

for any $\phi_h \in \Phi_h$. Therefore we have a partial orthogonality

$$(A(\tilde{\sigma} - \sigma_h), \mathbf{CurlCurl}\phi_h) = 0, \quad \forall\, \phi_h \in \Phi_h. \tag{3.4}$$

3.3 Upper bound

Let S_h^5 denote the Argyris finite element space, which consists of C^1 piecewise polynomials of degree less than or equal to 5, i.e.,

$$\begin{aligned} S_h^5 := \{v \in L^2(\bar{\Omega}) : v\,|_K \in P_5(K),\ \forall\, K \in \mathcal{T}_h,\ &v \text{ and its all first and second} \\ &\text{derivatives are continuous at the vertices, } v \text{ is continuous} \\ &\text{along the normal direction at the edge midpoints}\}. \end{aligned}$$

Following [23, 37], we can define a quasi-interpolation operator $I_h : H^2(\Omega) \to S_h^5$, which preserves the values of the function at all vertices of $\mathcal{T}_h$. On each element $K \in \mathcal{T}_h$, for any $v \in H^2(\Omega)$, $I_h v\,|_K \in P_5(K)$ and it satisfies

- $I_h v\,|_K(a_{i,K}) = v(a_{i,K})$, $1 \leqslant i \leqslant 3$;
- $\partial_{x_j}(I_h v\,|_K)(a_{i,K}) = \mathcal{N}_h^{-1}(a_{i,K}) \sum_{K' \in S(a_{i,K})} \partial_{x_j}(P_h v\,|_{K'})(a_{i,K})$, $1 \leqslant i \leqslant 3$, $j = 1, 2$;
- $\partial^2_{x_j x_l}(I_h v\,|_K)(a_{i,K}) = \mathcal{N}_h^{-1}(a_{i,K}) \sum_{K' \in S(a_{i,K})} \partial^2_{x_j x_l}(P_h v\,|_{K'})(a_{i,K})$, $1 \leqslant i \leqslant 3$, $1 \leqslant j \leqslant l \leqslant 2$;
- $\partial_\nu(I_h v\,|_K)(a_{3+i,K}) = \mathcal{N}_h^{-1}(a_{3+i,K}) \sum_{K' \in S(a_{3+i,K})} \partial_\nu(P_h v\,|_{K'})(a_{3+i,K})$, $1 \leqslant i \leqslant 3$,

where $a_{i,K}, 1 \leqslant i \leqslant 3$, are the vertices of K, $a_{3+i,K}, 1 \leqslant i \leqslant 3$, are the edge midpoints of K, ν is the edge outer normal of the element K at the edge midpoint,

$$S(a_{i,K}) := \bigcup\{K \in \mathcal{T}_h : a_{i,K} \in K\}$$

and

$$\mathcal{N}_h(a_{i,K}) := \mathrm{card}\{K : K \in S(a_{i,K})\},$$

P_h is the L^2 projection operator from $L^2(\Omega)$ onto the discontinuous finite element space of polynomial of degree $\leqslant 5$ on $\mathcal{T}_h$. It is obvious that the interpolation operator I_h is uniquely determined by the above degrees of freedom. Furthermore, I_h is a projection, i.e.,

$$I_h v = v, \quad \forall\, v \in S_h^5, \tag{3.5}$$

and it preserves the value of the function at vertices for any $v \in H^2(\Omega)$, i.e.,

$$I_h v(a_{i,K}) = v(a_{i,K}), \quad \forall\, K \in \mathcal{T}_h, \quad 1 \leqslant i \leqslant 3. \tag{3.6}$$

A similar scaling argument to that in [23, 37] gives the following interpolation estimates:

$$|v - I_h v|_{m,K} \lesssim h_K^{2-m} |v|_{2,S_K}, \quad 0 \leqslant m \leqslant 2, \quad \forall\, K \in \mathcal{T}_h, \tag{3.7}$$

$$|v - I_h v|_{m,e} \lesssim h_e^{2-m-\frac{1}{2}} |v|_{2,S_e}, \quad 0 \leqslant m \leqslant 1, \quad \forall\, e \in \mathcal{E}_h, \tag{3.8}$$

where $S_K = \bigcup\{K_i \in \mathcal{T}_h : K_i \cap K \neq \emptyset\}$ and $S_e = \bigcup\{K_i \in \mathcal{T}_h : K_i \cap e \neq \emptyset\}$.

Applying the Helmholtz decomposition to the error $\tilde{\sigma} - \sigma_h$, we have

$$\tilde{\sigma} - \sigma_h = \mathcal{C}\varepsilon(v) + \mathbf{CurlCurl}\phi = \mathbf{CurlCurl}\phi \tag{3.9}$$

and

$$\|\mathbf{CurlCurl}\phi\|_A = \|\tilde{\sigma} - \sigma_h\|_A, \tag{3.10}$$

where $\phi \in H^2(\Omega)/P_1(\Omega)$. It follows that

$$\|\tilde{\sigma} - \sigma_h\|_A^2 = (A(\tilde{\sigma} - \sigma_h), \mathbf{CurlCurl}\phi).$$

Since $\mathbf{CurlCurl}(I_h\phi) \in \Sigma_h$, by the orthogonality (3.4) and the equation (3.3),

$$\begin{aligned}(A(\tilde{\sigma} - \sigma_h), \mathbf{CurlCurl}\phi) &= (A(\tilde{\sigma} - \sigma_h), \mathbf{CurlCurl}(\phi - I_h\phi)) \\ &= -(A\sigma_h, \mathbf{CurlCurl}(\phi - I_h\phi)).\end{aligned}$$

An integration by parts gives

$$\begin{aligned}&(A\sigma_h, \mathbf{CurlCurl}(\phi - I_h\phi)) \\ &\quad = -\sum_{K\in\mathcal{T}_h}(\mathrm{curl}(A\sigma_h), \mathbf{Curl}(\phi - I_h\phi))_K + \sum_{K\in\mathcal{T}_h}\langle(A\sigma_h)t, \mathbf{Curl}(\phi - I_h\phi)\rangle_{\partial K} \\ &\quad = \sum_{K\in\mathcal{T}_h}(\mathrm{curlcurl}(A\sigma_h), \phi - I_h\phi)_K + \sum_{K\in\mathcal{T}_h}\langle(A\sigma_h)t, \mathbf{Curl}(\phi - I_h\phi)\rangle_{\partial K} \\ &\qquad - \sum_{K\in\mathcal{T}_h}\langle\mathrm{curl}(A\sigma_h)\cdot t, \phi - I_h\phi\rangle_{\partial K}.\end{aligned} \tag{3.11}$$

The second term of the right-hand side can be rewritten as

$$\begin{aligned}\sum_{K\in\mathcal{T}_h}\langle A\sigma_h t, \mathbf{Curl}(\phi - I_h\phi)\rangle_{\partial K} &= \sum_{K\in\mathcal{T}_h}\langle(A\sigma_h)t\cdot t, \mathbf{Curl}(\phi - I_h\phi)\cdot t\rangle_{\partial K} \\ &\quad + \sum_{K\in\mathcal{T}_h}\langle(A\sigma_h t)\cdot\nu, \mathbf{Curl}(\phi - I_h\phi)\cdot\nu\rangle_{\partial K}.\end{aligned}$$

Since the compliance tensor A is symmetric and continuous, $(A\sigma_h t)\cdot\nu = (A\sigma_h\nu)\cdot t = (t^{\mathrm{T}}\sigma_h\nu)/(2\mu)$ and $(A\sigma_h t)\cdot\nu$ is continuous across the interior element edge, which implies

$$\begin{aligned}\sum_{K\in\mathcal{T}_h}\langle(A\sigma_h t)\cdot\nu, \mathbf{Curl}(\phi - I_h\phi)\cdot\nu\rangle_{\partial K} &= -\sum_{e\in\mathcal{E}_h(\Gamma)}\langle(A\sigma_h t_e)\cdot\nu_e, \partial_{t_e}(\phi - I_h\phi)\rangle_e \\ &= \sum_{e\in\mathcal{E}_h(\Gamma)}\langle\partial_{t_e}((A\sigma_h t_e)\cdot\nu_e), \phi - I_h\phi\rangle_e,\end{aligned}$$

where the fact $\phi - I_h\phi$ vanishing at the vertices (3.6) is used. So

$$\begin{aligned}\sum_{K\in\mathcal{T}_h}\langle A\sigma_h t, \mathbf{Curl}(\phi - I_h\phi)\rangle_{\partial K} &= \sum_{e\in\mathcal{E}_h(\Omega)}\langle[(A\sigma_h t_e)\cdot t_e]_e, \partial_{\nu_e}(\phi - I_h\phi)\rangle_e \\ &\quad + \sum_{e\in\mathcal{E}_h(\Gamma)}\langle(A\sigma_h t_e)\cdot t_e, \partial_{\nu_e}(\phi - I_h\phi)\rangle_e \\ &\quad + \sum_{e\in\mathcal{E}_h(\Gamma)}\langle\partial_{t_e}((A\sigma_h t_e)\cdot\nu_e), \phi - I_h\phi\rangle_e.\end{aligned}$$

Substituting it into (3.11), we get

$$\begin{aligned}(A\sigma_h, \mathbf{CurlCurl}(\phi - I_h\phi)) &= \sum_{K\in\mathcal{T}_h}(\mathrm{curl}\,\mathrm{curl}\,(A\sigma_h), \phi - I_h\phi)_K \\ &\quad + \sum_{e\in\mathcal{E}_h(\Omega)}\langle[(A\sigma_h t_e)\cdot t_e]_e, \partial_{\nu_e}(\phi - I_h\phi)\rangle_e \\ &\quad - \sum_{e\in\mathcal{E}_h(\Omega)}\langle[\mathrm{curl}(A\sigma_h)\cdot t_e]_e, \phi - I_h\phi\rangle_e\end{aligned}$$

$$+\sum_{e\in\mathcal{E}_h(\Gamma)}\langle (A\sigma_h t_e)\cdot t_e, \partial_{\nu_e}(\phi - I_h\phi)\rangle_e$$
$$+\sum_{e\in\mathcal{E}_h(\Gamma)}\langle \partial_{t_e}((A\sigma_h t_e)\cdot \nu_e) - \operatorname{curl}(A\sigma_h)\cdot t_e, \phi - I_h\phi\rangle_e$$

and

$$\begin{aligned}\|\tilde\sigma - \sigma_h\|_A^2 &= (A(\tilde\sigma - \sigma_h), \mathbf{CurlCurl}\phi)\\ &\lesssim \bigg[\sum_{K\in\mathcal{T}_h} h_K^4\|\operatorname{curlcurl}(A\sigma_h)\|_{0,K}^2 + \sum_{e\in\mathcal{E}_h}(h_e\|\mathcal{J}_{e,1}\|_{0,e}^2 + h_e^3\|\mathcal{J}_{e,2}\|_{0,e}^2)\bigg]^{\frac12}|\phi|_2\\ &\lesssim \bigg[\sum_{K\in\mathcal{T}_h}\eta_K^2(\sigma_h) + \sum_{e\in\mathcal{E}_h}\eta_e^2(\sigma_h)\bigg]^{\frac12}\|\mathbf{CurlCurl}\phi\|_0.\end{aligned} \tag{3.12}$$

By [14], the ϕ defined in (3.9) satisfies that $\operatorname{div}(\mathbf{CurlCurl}\phi) = 0$ and

$$\int_\Omega \operatorname{tr}(\mathbf{CurlCurl}\phi)dx = \int_\Omega \operatorname{tr}(\tilde\sigma - \sigma_h)dx = 0.$$

Using [11, Proposition 9.1.1], we get

$$\|\mathbf{CurlCurl}\phi\|_0 \leqslant C\|\mathbf{CurlCurl}\phi\|_A,$$

where the constant C is independent of the Lamé constant λ. Combining this with (3.10) and (3.12), we obtain

$$\|\tilde\sigma - \sigma_h\|_A \lesssim \bigg[\sum_{K\in\mathcal{T}_h}\eta_K^2(\sigma_h) + \sum_{e\in\mathcal{E}_h}\eta_e^2(\sigma_h)\bigg]^{\frac12}.$$

Together with the triangle inequality and the perturbation result (3.2), we get the desired error bound

$$\begin{aligned}\|\sigma - \sigma_h\|_A &\leqslant \|\sigma - \tilde\sigma\|_A + \|\tilde\sigma - \sigma_h\|_A\\ &\lesssim \bigg[\sum_{K\in\mathcal{T}_h}\eta_K^2(\sigma_h) + \sum_{e\in\mathcal{E}_h}\eta_e^2(\sigma_h)\bigg]^{\frac12} + \operatorname{osc}(f, \mathcal{T}_h).\end{aligned}$$

In summary, we obtain the following upper bound estimation.

Theorem 3.2 (Reliability of the error estimator)**.** *Let (σ, u) be the solution of the mixed formulation* (1.1) *and (σ_h, u_h) be the solution of the mixed finite element method* (2.1)*. If the compliance tensor A is continuous, there exists a positive constant C_1 depending only on the shape-regularity of the triangulation and the polynomial degree k such that*

$$\|\sigma - \sigma_h\|_A \leqslant C_1(\eta(\sigma_h, \mathcal{T}_h) + \operatorname{osc}(f, \mathcal{T}_h)). \tag{3.13}$$

Remark 3.3. When A is discontinuous, we can modify $\eta(\sigma_h, \mathcal{T}_h)$ as follows:

$$\begin{aligned}\eta^2(\sigma_h, \mathcal{T}_h) := &\sum_{K\in\mathcal{T}_h} h_K^4\|\operatorname{curl}\operatorname{curl}(A\sigma_h)\|_{0,K}^2 + \sum_{e\in\mathcal{E}_h} h_e\|[(A\sigma_h)t_e\cdot t_e]\|_{0,e}^2\\ &+ \sum_{e\in\mathcal{E}_h} h_e^3\|[\operatorname{curl}(A\sigma_h)\cdot t_e - \partial_{t_e}((A\sigma_h)t_e\cdot\nu_e)]\|_{0,e}^2.\end{aligned}$$

Compared with the case of continuous coefficient A, this estimator includes an additional term, the jump of $\partial_{t_e}((A\sigma_h)t_e\cdot\nu_e)$ on all interior edges, owing to the discontinuity of the matrix A. Similarly, we can prove the reliability of the estimator

$$\|\sigma - \sigma_h\|_A \lesssim \eta(\sigma_h, \mathcal{T}_h) + \operatorname{osc}(f, \mathcal{T}_h).$$

Remark 3.4. By [11, Proposition 9.1.1], it holds

$$\|\tau\|_0 \lesssim \|\tau\|_A + \|\operatorname{div}\tau\|_{-1}, \quad \forall\, \tau \in \hat{\Sigma},$$

where $\hat{\Sigma} := \{\tau \in \Sigma : (\mathrm{tr}\tau, 1) = 0\}$ with tr being the trace operator of matrix. Then we also have from (3.13) and the fact that $\|f - f_h\|_{-1} \lesssim \mathrm{osc}(f, \mathcal{T}_h)$,

$$\|\sigma - \sigma_h\|_0 \lesssim \|\sigma - \sigma_h\|_A + \|\operatorname{div}(\sigma - \sigma_h)\|_{-1} \lesssim \eta(\sigma_h, \mathcal{T}_h) + \mathrm{osc}(f, \mathcal{T}_h),$$

i.e., we can control the L^2 norm of the stress with constant independent of the Lamé constant λ.

3.4 Lower bound

We shall follow Alonso [2] to prove the efficiency of the error estimator defined in (3.1). Similar to [2], we need the following lemma.

Lemma 3.5. *For any $K \in \mathcal{T}_h$, given $p_K \in L^2(K)$, $q_e \in L^2(e)$, $r_e \in L^2(e)$, $e \in \partial K$, there exists a unique $\psi_K \in P_{k+5}(K)$, $k \geqslant 1$, satisfying that*

$$\begin{cases} (\psi_K, v) = (p_K, v)_K & \text{for any} \quad v \in P_{k-1}(K), \\ \langle \psi_K, s\rangle_e = \langle q_e, s\rangle_e & \text{for any} \quad s \in P_{k-1}(e), \\ \langle \partial_\nu \psi_K, s\rangle_e = \langle r_e, s\rangle_e & \text{for any} \quad s \in P_k(e), \\ \partial^\alpha \psi_K(P) = 0, \quad |\alpha| \leqslant 2 & \text{for any vertex} \quad P \in K, \end{cases} \tag{3.14}$$

where $P_k(e)$ denotes the spaces of polynomial of degree less than or equal to k on edge e. Moreover, it holds that

$$\|\psi_K\|_{0,K}^2 \lesssim \|p_K\|_{0,K}^2 + \sum_{e\in\partial K} (h_e\|q_e\|_{0,e}^2 + h_e^3\|r_e\|_{0,e}^2). \tag{3.15}$$

Proof. Similar to [36], such a function ψ_K is determined uniquely by the above degrees of freedoms. A standard homogeneity argument gives (3.15). □

Theorem 3.6 (Efficiency of the error estimator). *Let (σ, u) be the solution of the mixed formulation (1.1) and (σ_h, u_h) be the solution of the mixed finite element method (2.1). If the compliance tensor A is continuous, there exists a positive constant C_2 depending only on the shape-regularity of the triangulations and the polynomial degree k such that*

$$C_2\eta(\sigma_h, \mathcal{T}_h) \leqslant \|\sigma - \sigma_h\|_A. \tag{3.16}$$

Proof. The estimator $\eta^2(\sigma_h, \mathcal{T}_h)$ can be rewritten as

$$\begin{aligned} \eta^2(\sigma_h, \mathcal{T}_h) = &\sum_{K\in\mathcal{T}_h} (\mathrm{curlcurl}(A\sigma_h), h_K^4 \mathrm{curlcurl}(A\sigma_h))_K \\ &+ \sum_{K\in\mathcal{T}_h}\sum_{e\in\partial K} \langle (A\sigma_h)t_e\cdot t_e,\, h_e\mathcal{J}_{e,1}\rangle_e \\ &+ \sum_{K\in\mathcal{T}_h}\sum_{e\in\partial K\cap\mathcal{E}_h(\Omega)} \langle \mathrm{curl}\,(A\sigma_h)\cdot t_e,\, h_e^3\mathcal{J}_{e,2}\rangle_e \\ &+ \sum_{K\in\mathcal{T}_h}\sum_{e\in\partial K\cap\mathcal{E}_h(\Gamma)} \langle \mathrm{curl}\,(A\sigma_h)\cdot t_e - \partial_{t_e}((A\sigma_h)t_e\cdot\nu_e), h_e^3\mathcal{J}_{e,2}\rangle_e. \end{aligned}$$

On each element $K \in \mathcal{T}_h$, we apply Lemma 3.5 for $p_K = h_K^4\mathrm{curlcurl}(A\sigma_h)|_K$, $q_e = -h_e^3\mathcal{J}_{e,2}$, $r_e = h_e\mathcal{J}_{e,1}$ for each edge $e \in \partial K$. Let $\psi|_K = \psi_K$, ψ is in fact in the high-order Argyris finite element space of degree $k+5$ ($k \geqslant 1$), and hence $\psi \in H^2(\Omega)$. Using (3.15), it follows that

$$\|\psi\|_{0,K}^2 \lesssim h_K^8\|\mathrm{curlcurl}(A\sigma_h)\|_{0,K}^2 + \sum_{e\in\partial K} (h_e^7\|\mathcal{J}_{e,2}\|_{0,e}^2 + h_e^5\|\mathcal{J}_{e,1}\|_{0,e}^2). \tag{3.17}$$

This, in conjunction with (3.14), yields

$$\begin{aligned}\eta^2(\sigma_h,\mathcal{T}_h)=&\sum_{K\in\mathcal{T}_h}(\operatorname{curlcurl}(A\sigma_h),\psi_K)_K\\&-\sum_{K\in\mathcal{T}_h}\sum_{e\in\partial K}\langle\operatorname{curl}(A\sigma_h)\cdot t_e,\psi_K\rangle_e\\&+\sum_{K\in\mathcal{T}_h}\sum_{e\in\partial K}\langle(A\sigma_h)t_e\cdot t_e,\partial_{\nu_e}\psi_K\rangle_e\\&+\sum_{K\in\mathcal{T}_h}\sum_{e\in\partial K\cap\mathcal{E}_h(\Gamma)}\langle\partial_{t_e}((A\sigma_h)t_e\cdot\nu_e),\psi_K\rangle_e.\end{aligned}\tag{3.18}$$

Since $(A\sigma_h)t_e\cdot\nu_e$ is continuous across the interior element edge e, $[A\sigma_h t_e\cdot\nu_e]_e=0$ on interior edges. Note that $\psi\in H^2(\Omega)$ and vanishes at the mesh vertices,

$$\begin{aligned}&\sum_{K\in\mathcal{T}_h}\sum_{e\in\partial K\cap\mathcal{E}_h(\Gamma)}\langle\partial_{t_e}((A\sigma_h)t_e\cdot\nu_e),\psi_K\rangle_e\\&\quad=-\sum_{K\in\mathcal{T}_h}\sum_{e\in\partial K\cap\mathcal{E}_h(\Gamma)}\langle(A\sigma_h)t_e\cdot\nu_e,\partial_{t_e}\psi_K\rangle_e\\&\quad=-\sum_{K\in\mathcal{T}_h}\sum_{e\in\partial K}\langle(A\sigma_h)t_e\cdot\nu_e,\partial_{t_e}\psi_K\rangle_e.\end{aligned}\tag{3.19}$$

Hence the last two terms of (3.18) become

$$\begin{aligned}&\sum_{K\in\mathcal{T}_h}\sum_{e\in\partial K}\langle(A\sigma_h)t_e\cdot t_e,\partial_{\nu_e}\psi_K\rangle_e+\sum_{K\in\mathcal{T}_h}\sum_{e\in\partial K\cap\mathcal{E}_h(\Gamma)}\langle\partial_{t_e}((A\sigma_h)t_e\cdot\nu_e),\psi_K\rangle_e\\&\quad=\sum_{K\in\mathcal{T}_h}\sum_{e\in\partial K}\langle(A\sigma_h)t_e\cdot t_e,\,\mathbf{Curl}\psi_K\cdot t_e\rangle_e-\sum_{K\in\mathcal{T}_h}\sum_{e\in\partial K}\langle(A\sigma_h)t_e\cdot\nu_e,-\mathbf{Curl}\psi_K\cdot\nu_e\rangle_e\\&\quad=\sum_{K\in\mathcal{T}_h}\sum_{e\in\partial K}\langle(A\sigma_h)t_e,\,\mathbf{Curl}\psi_K\rangle_e.\end{aligned}\tag{3.20}$$

Substituting (3.20) into (3.18) leads to

$$\eta^2(\sigma_h,\mathcal{T}_h)=\sum_{K\in\mathcal{T}_h}\bigg((\operatorname{curlcurl}(A\sigma_h),\psi_K)_K-\sum_{e\in\partial K}\langle\operatorname{curl}(A\sigma_h)\cdot t_e,\psi_K\rangle_e+\sum_{e\in\partial K}\langle(A\sigma_h)t_e,\mathbf{Curl}\psi_K\rangle_e\bigg).$$

Integrating the first term by parts twice,

$$\begin{aligned}\eta^2(\sigma_h,\mathcal{T}_h)&=\sum_{K\in\mathcal{T}_h}(A\sigma_h,\,\mathbf{CurlCurl}\psi_K)_K\\&=\sum_{K\in\mathcal{T}_h}(A(\sigma_h-\sigma),\mathbf{CurlCurl}\psi_K)_K\\&\lesssim\|\sigma-\sigma_h\|_A\bigg(\sum_{K\in\mathcal{T}_h}h_K^{-4}\|\psi\|_{0,K}^2\bigg)^{\frac{1}{2}},\end{aligned}$$

where $\mathbf{CurlCurl}\psi\in\Sigma$ and the inverse inequality are used. By (3.17),

$$\begin{aligned}\sum_{K\in\mathcal{T}_h}h_K^{-4}\|\psi\|_{0,K}^2&\lesssim\sum_{K\in\mathcal{T}_h}h_K^4\|\operatorname{curl}\operatorname{curl}(A\sigma_h)\|_{0,K}^2+\sum_{e\in\mathcal{E}_h}(h_e\|\mathcal{J}_{e,1}\|_{0,e}^2+h_e^3\|\mathcal{J}_{e,2}\|_{0,e}^2)\\&\mathrel{\widehat{=}}\eta^2(\sigma_h,\mathcal{T}_h).\end{aligned}$$

Combining the above two inequalities, we have that

$$\eta(\sigma_h,\mathcal{T}_h)\lesssim\|\sigma-\sigma_h\|_A.$$

This completes the proof. □

Remark 3.7. For discontinuous A and the modified error estimator in Remark 3.3, efficiency can be also proved using a similar argument.

4 A posteriori error estimation for mixed boundary problems

The *a posteriori* error estimation for the linear elasticity problems with the homogeneous Dirichlet boundary condition can be generalized to problems with mixed boundary conditions. In this section, we will discuss the following linear elasticity problems with mixed boundary conditions. Let $\Omega \subset \mathbb{R}^2$ be a bounded polygonal domain with boundary $\Gamma := \partial\Omega = \Gamma_D \cup \Gamma_N$, $\Gamma_D \cap \Gamma_N = \emptyset$, $\Gamma_N \neq \emptyset$. Given data $f \in L^2(\Omega;\mathbb{R}^2)$, $u_D \in H^1(\Omega;\mathbb{R}^2)$ and $g \in L^2(\Gamma_N;\mathbb{R}^2)$, seek the solution $(\sigma, u) \in \Sigma_g \times V$, such that

$$\begin{cases} (A\sigma,\tau) + (\mathrm{div}\tau, u) = \langle u_D, \tau\nu\rangle_{\Gamma_D} & \text{for all } \ \tau \in \Sigma_0, \\ (\mathrm{div}\sigma, v) = (f, v) & \text{for all } \ v \in V, \end{cases} \tag{4.1}$$

where

$$\Sigma_0 := \left\{ \sigma \in H(\mathrm{div},\Omega;\mathbb{S}) \,\middle|\, \int_{\Gamma_N} \psi\cdot(\sigma\nu)ds = 0, \text{ for all } \psi \in \mathcal{D}(\Gamma_N;\mathbb{R}^2) \right\},$$
$$\Sigma_g := \left\{ \sigma \in H(\mathrm{div},\Omega;\mathbb{S}) \,\middle|\, \int_{\Gamma_N} \psi\cdot(\sigma\nu)ds = \int_{\Gamma_N} \psi\cdot g ds, \text{ for all } \psi \in \mathcal{D}(\Gamma_N;\mathbb{R}^2) \right\},$$

where $\mathcal{D}$ denotes the space of test functions. Let $\Sigma_{0,h} := \Sigma_0 \cap \Sigma_h$, $\Sigma_{g,h} := \Sigma_g \cap \Sigma_h$, the mixed finite element method seeks $(\sigma_h, u_h) \in \Sigma_{g,h} \times V_h$, such that

$$\begin{cases} (A\sigma_h,\tau_h) + (\mathrm{div}\tau_h, u_h) = \langle u_D, \tau_h\nu\rangle_{\Gamma_D} & \text{for all } \ \tau_h \in \Sigma_{0,h}, \\ (\mathrm{div}\sigma_h, v_h) = (f, v_h) & \text{for all } \ v_h \in V_h. \end{cases} \tag{4.2}$$

We modify the *a posterior* error estimator defined in Section 3 as follows:

$$\eta^2(\sigma_h,\mathcal{T}_h) := \sum_{K\in\mathcal{T}_h} \eta_K^2(\sigma_h) + \sum_{e\in\mathcal{E}_h} \eta_e^2(\sigma_h),$$

where

$$\eta_K^2(\sigma_h) := h_K^4 \|\mathrm{curlcurl}(A\sigma_h)\|_{0,K}^2, \quad \eta_e^2(\sigma_h) := h_e\|\mathcal{J}_{e,1}\|_{0,e}^2 + h_e^3\|\mathcal{J}_{e,2}\|_{0,e}^2,$$
$$\mathcal{J}_{e,1} := \begin{cases} [(A\sigma_h)t_e\cdot t_e]_e, & \text{if } e \in \mathcal{E}_h(\Omega), \\ ((A\sigma_h)t_e\cdot t_e - \partial_{t_e}(u_D\cdot t_e))\,|_e, & \text{if } e \in \mathcal{E}_h(\Gamma_D), \end{cases}$$
$$\mathcal{J}_{e,2} := \begin{cases} [\mathrm{curl}(A\sigma_h)\cdot t_e]_e, & \text{if } e \in \mathcal{E}_h(\Omega), \\ (\mathrm{curl}(A\sigma_h)\cdot t_e + \partial_{t_e t_e}(u_D\cdot\nu) - \partial_{t_e}((A\sigma_h)t_e\cdot\nu_e))\,|_e, & \text{if } e \in \mathcal{E}_h(\Gamma_D), \end{cases}$$

where $\mathcal{E}_h(\Gamma_D)$ is the collection of element edges on the Dirichlet boundary.

Similar to Section 3, we can prove the reliability and efficiency of this *a posteriori* error estimator.

Theorem 4.1 (Reliability and efficiency of the error estimator). *Let (σ, u) be the solution of the mixed formulation (4.1) and (σ_h, u_h) be the solution of the mixed finite element method (4.2). If the compliance tensor A is continuous, there exist positive constants C_3 and C_4 depending only on the shape-regularity of the triangulation and the polynomial degree k such that*

$$\|\sigma - \sigma_h\|_A \leqslant C_3(\eta(\sigma_h,\mathcal{T}_h) + \mathrm{osc}(f,\mathcal{T}_h) + \mathrm{osc}(g,\mathcal{E}_h(\Gamma_N))), \tag{4.3}$$

and

$$C_4\eta(\sigma_h,\mathcal{T}_h) \leqslant \|\sigma - \sigma_h\|_A + \mathrm{osc}(u_D,\mathcal{E}_h(\Gamma_D)), \tag{4.4}$$

where the data oscillations for the Dirichlet boundary u_D and the Neumann boundary condition g are defined as

$$\mathrm{osc}(g,\mathcal{E}_h(\Gamma_N))^2 := \sum_{e\in\mathcal{E}_h(\Gamma_N)} h_e\|g - g_h\|_{0,e}^2,$$

$$\operatorname{osc}(u_D,\mathcal{E}_h(\Gamma_D))^2 := \sum_{e\in\mathcal{E}_h(\Gamma_D)} h_e\|\partial_{t_e}(u_D\cdot t_e)-\partial_{t_e}(u_{D,h}\cdot t_e)\|_{0,e}^2 + \sum_{e\in\mathcal{E}_h(\Gamma_D)} h_e^3\|\partial_{t_et_e}(u_D\cdot \nu_e)-\partial_{t_et_e}(u_{D,h}\cdot \nu_e)\|_{0,e}^2,$$

where g_h is the piecewise L^2 projection of g onto $P_k(\mathcal{E}_h(\Gamma_N),\mathbb{R}^2)$ and $u_{D,h}$ is the piecewise L^2 projection of u_D onto $P_k(\mathcal{E}_h(\Gamma_D),\mathbb{R}^2)$.

5 A posteriori error estimation for displacement

In this section, we shall discuss the *a posteriori* error estimate for a superconvergent postprocessed displacement recently constructed in [20]. The key points of the theoretical analysis involve the discrete inf-sup condition and the norm equivalence on $H^1(\mathcal{T}_h;\mathbb{R}^2)$ developed in [20], and the *a posteriori* error estimates (3.13) and (3.16). Here, the broken space

$$H^1(\mathcal{T}_h;\mathbb{R}^2) := \{v\in L^2(\Omega;\mathbb{R}^2) : v\,|_K\in H^1(K;\mathbb{R}^2),\ \forall\, K\in\mathcal{T}_h\}.$$

For any $v\in H^1(\mathcal{T}_h;\mathbb{R}^2)$, define the following mesh dependent norm

$$|v|_{1,h}^2 := \|\varepsilon_h(v)\|_0^2 + \sum_{e\in\mathcal{E}_h} h_e^{-1}\|[v]\|_{0,e}^2,$$

where $\varepsilon_h(v)\,|_K = \varepsilon(v\,|_K)$ for any $K\in\mathcal{T}_h$.

We first recall the superconvergent postprocessed displacement from (σ_h,u_h) developed in [20]. To this end, let

$$V_h^* := \{v\in L^2(\Omega;\mathbb{R}^2) : v\,|_K\in P_{k+1}(K;\mathbb{R}^2),\ \forall\, K\in\mathcal{T}_h\}.$$

Then a postprocessed displacement is defined as follows (see [12, 20, 35]): find $u_h^*\in V_h^*$ such that

$$(u_h^*,v)_K = (u_h,v)_K,\quad \forall\, v\in P_{k-1}(K;\mathbb{R}^2), \tag{5.1}$$

$$(\varepsilon(u_h^*),\varepsilon(w))_K = (A\sigma_h,\varepsilon(w))_K,\quad \forall\, w\in(I-Q_h)V_h^*\,|_K, \tag{5.2}$$

for any $K\in\mathcal{T}_h$.

We recall the following two useful results (see [20]): the discrete inf-sup condition

$$|v_h|_{1,h} \lesssim \sup_{0\neq\tau_h\in\Sigma_h}\frac{(\operatorname{div}\tau_h,v_h)}{\|\tau_h\|_0},\quad \forall\, v_h\in V_h, \tag{5.3}$$

and norm equivalence

$$|v-Q_hv|_{1,h} \eqsim \|\varepsilon_h(v-Q_hv)\|_0,\quad \forall\, v\in H^1(\mathcal{T}_h;\mathbb{R}^2). \tag{5.4}$$

Theorem 5.1. *Let (σ,u) be the solution of the mixed formulation (1.1), (σ_h,u_h) be the solution of the mixed finite element method (2.1), and u_h^* be the postprocessed displacement defined by (5.1)–(5.2). Then we have*

$$\|\sigma-\sigma_h\|_A + |u-u_h^*|_{1,h} \lesssim \eta(\sigma_h,\mathcal{T}_h) + \|A\sigma_h-\varepsilon_h(u_h^*)\|_0 + \operatorname{osc}(f,\mathcal{T}_h), \tag{5.5}$$

$$\eta(\sigma_h,\mathcal{T}_h) + \|A\sigma_h-\varepsilon_h(u_h^*)\|_0 \lesssim \|\sigma-\sigma_h\|_A + |u-u_h^*|_{1,h}. \tag{5.6}$$

Proof. Using the discrete inf-sup condition (5.3) with $v_h = Q_h(u-u_h^*)$, (5.1), the first equation of (1.1) and (2.1), we get

$$\begin{aligned}|Q_h(u-u_h^*)|_{1,h} &\lesssim \sup_{0\neq\tau_h\in\Sigma_h}\frac{(\operatorname{div}\tau_h,Q_h(u-u_h^*))}{\|\tau_h\|_0}\\ &= \sup_{0\neq\tau_h\in\Sigma_h}\frac{(\operatorname{div}\tau_h,u-u_h)}{\|\tau_h\|_0}\end{aligned}$$

$$
\begin{aligned}
&= \sup_{0\neq\tau_h\in\Sigma_h} \frac{(A(\sigma-\sigma_h),\tau_h)}{\|\tau_h\|_0} \\
&\leqslant \|A(\sigma-\sigma_h)\|_0.
\end{aligned}
$$

Choosing $v = u - u_h^*$ in (5.4), we have

$$
\begin{aligned}
|v - Q_h v|_{1,h} \eqsim \|\varepsilon_h(v - Q_h v)\|_0 &\leqslant \|\varepsilon_h(u-u_h^*)\|_0 + |Q_h(u-u_h^*)|_{1,h} \\
&= \|A\sigma - \varepsilon_h(u_h^*)\|_0 + |Q_h(u-u_h^*)|_{1,h} \\
&\lesssim \|A\sigma_h - \varepsilon_h(u_h^*)\|_0 + \|A(\sigma-\sigma_h)\|_0.
\end{aligned}
$$

Then it follows from the last two inequalities that

$$
|u-u_h^*|_{1,h} \lesssim \|A\sigma_h - \varepsilon_h(u_h^*)\|_0 + \|A(\sigma-\sigma_h)\|_0,
$$

which combined with (3.13) implies (5.5).

Next, we prove the efficiency (5.6). By the triangle inequality,

$$
\begin{aligned}
\|A\sigma_h - \varepsilon_h(u_h^*)\|_0 &\leqslant \|A(\sigma-\sigma_h)\|_0 + \|A\sigma - \varepsilon_h(u_h^*)\|_0 \\
&= \|A(\sigma-\sigma_h)\|_0 + \|\varepsilon_h(u-u_h^*)\|_0 \\
&\lesssim \|\sigma-\sigma_h\|_A + |u-u_h^*|_{1,h}.
\end{aligned}
$$

Therefore we can end the proof by using (3.16). □

6 Numerical experiments

We will testify the *a posteriori* error estimator by some numerical examples in this section.

In the first example, let $\Omega = (0,1)^2$, $k=3$, $\mu=1$, the right-hand side

$$
f(x,y) = \pi^3 \begin{pmatrix} -\sin(2\pi y)(2\cos(2\pi x)-1) \\ \sin(2\pi x)(2\cos(2\pi y)-1) \end{pmatrix},
$$

and the exact solution (see [16, Section 5.2])

$$
u(x,y) = \frac{\pi}{2} \begin{pmatrix} \sin^2(\pi x)\sin(2\pi y) \\ -\sin^2(\pi y)\sin(2\pi x) \end{pmatrix}.
$$

We subdivide Ω by a uniform triangular mesh. The *a priori* and *a posteriori* error estimates for $\lambda = 10$ and $\lambda = 10{,}000$ are listed in Tables 1 and 2, from which we can see that the convergence rates of $\|\sigma-\sigma_h\|_A$, $\|\nabla_h(u-u_h^*)\|_0$, $\eta(\sigma_h,\mathcal{T}_h)$ and $\|A\sigma_h - \varepsilon_h(u_h^*)\|_0$ are all $O(h^4)$. Hence, the *a posteriori* error estimators $\eta(\sigma_h,\mathcal{T}_h)$ and $\eta(\sigma_h,\mathcal{T}_h)+\|A\sigma_h-\varepsilon_h(u_h^*)\|_0$ are both uniformly reliable and efficient with respect to the mesh size h and λ for smooth solutions.

Table 1 Numerical errors for the first example when $\lambda = 10$

h	$\|\sigma-\sigma_h\|_A$	Order	$\|\nabla_h(u-u_h^*)\|_0$	Order	$\eta(\sigma_h,\mathcal{T}_h)$	Order	$\|A\sigma_h-\varepsilon_h(u_h^*)\|_0$	Order
2^{-1}	6.6998E−01	–	7.9544E−01	–	1.6615E+01	–	4.0073E−02	–
2^{-2}	5.2451E−02	3.68	6.0585E−02	3.71	1.3585E+00	3.61	9.3899E−03	2.09
2^{-3}	3.6139E−03	3.86	4.5839E−03	3.72	1.0918E−01	3.64	7.1387E−04	3.72
2^{-4}	2.2714E−04	3.99	3.0676E−04	3.90	7.4510E−03	3.87	4.5925E−05	3.96
2^{-5}	1.4193E−05	4.00	1.9600E−05	3.97	4.7919E−04	3.96	2.8824E−06	3.99
2^{-6}	8.8742E−07	4.00	1.2347E−06	3.99	3.0263E−05	3.99	1.8040E−07	4.00
2^{-7}	5.5567E−08	4.00	7.7435E−08	3.99	1.8992E−06	3.99	1.1306E−08	4.00

Table 2 Numerical errors for the first example when $\lambda = 10{,}000$

h	$\|\sigma - \sigma_h\|_A$	Order	$\|\nabla_h(u - u_h^*)\|_0$	Order	$\eta(\sigma_h, \mathcal{T}_h)$	Order	$\|A\sigma_h - \varepsilon_h(u_h^*)\|_0$	Order
2^{-1}	6.6096E−01	–	7.7905E−01	–	1.6050E+01	–	4.3292E−02	–
2^{-2}	5.1630E−02	3.68	5.8762E−02	3.73	1.3066E+00	3.62	9.0182E−03	2.26
2^{-3}	3.5430E−03	3.87	4.3977E−03	3.74	1.0508E−01	3.64	6.8780E−04	3.71
2^{-4}	2.2220E−04	4.00	2.9277E−04	3.91	7.1542E−03	3.88	4.4330E−05	3.96
2^{-5}	1.3873E−05	4.00	1.8668E−05	3.97	4.5947E−04	3.96	2.7853E−06	3.99
2^{-6}	8.6708E−07	4.00	1.1751E−06	3.99	2.8998E−05	3.99	1.7442E−07	4.00
2^{-7}	5.4210E−08	4.00	7.3695E−08	4.00	1.8195E−06	3.99	1.0922E−08	4.00

Algorithm 1 Adaptive algorithm for the mixed finite element method (2.1)

Given a parameter $0 < \vartheta < 1$ and an initial mesh $\mathcal{T}_0$. Set $m := 0$.

1. **SOLVE**: Solve the mixed finite element method (2.1) on $\mathcal{T}_m$ for the discrete solution $(\sigma_m, u_m) \in \Sigma_m \times V_m$.
2. **ESTIMATE**: Compute the error indicator $\eta^2(\sigma_m, \mathcal{T}_m)$ piecewise.
3. **MARK**: Mark a set $\mathcal{S}_m \subset \mathcal{T}_m$ with minimal cardinality by Dörfler marking such that
$$\eta^2(\sigma_m, \mathcal{S}_m) \geqslant \vartheta \eta^2(\sigma_m, \mathcal{T}_m).$$
4. **REFINE**: Refine each triangle K with at least one edge in $\mathcal{S}_m$ by the newest vertex bisection to get $\mathcal{T}_{m+1}$.
5. Set $m := m + 1$ and go to Step 1.

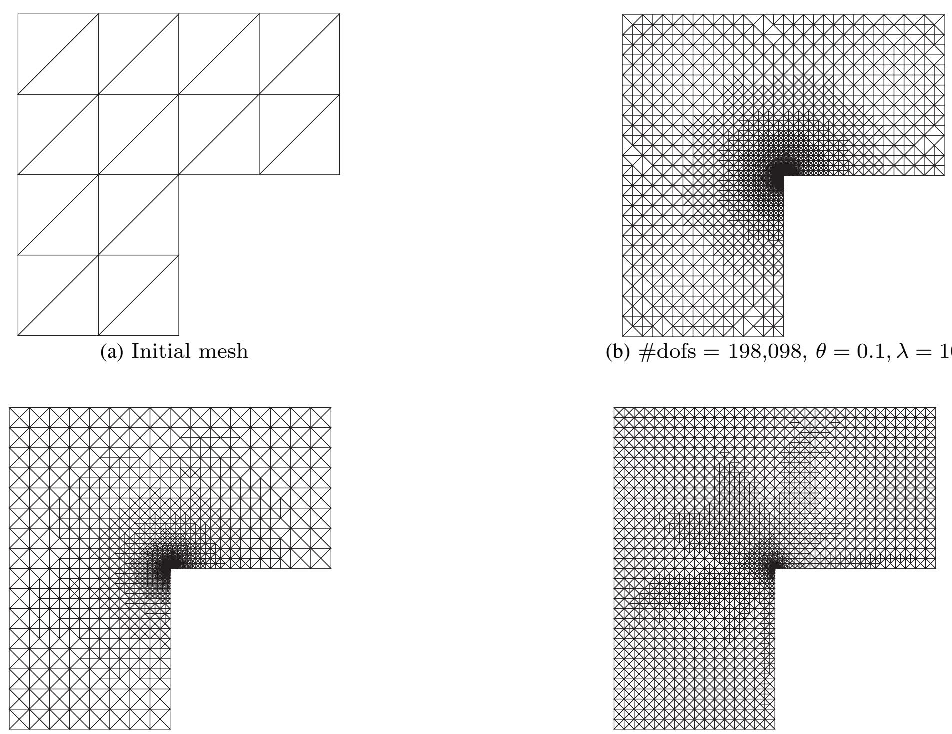

(a) Initial mesh

(b) #dofs = 198,098, $\theta = 0.1, \lambda = 10$

(c) #dofs = 129,624, $\theta = 0.2, \lambda = 10$

(d) #dofs = 138,323, $\theta = 0.2, \lambda = 10{,}000$

Figure 1 Meshes generated in Algorithm 1 with different θ and λ for Example 2

Next, we use the *a posteriori* error estimator $\eta(\sigma_h, \mathcal{T}_h)$ to design an adaptive mixed finite element method, i.e., Algorithm 1. The approximate block factorization preconditioner with the generalized minimal residual method (GMRES, see [20]) is adopted in the SOLVE part of Algorithm 1, which is verified to be highly efficient and robust even on adaptive meshes by our numerical examples.

Now we construct a problem with singularity in the solution to test Algorithm 1. Set L-shaped domain

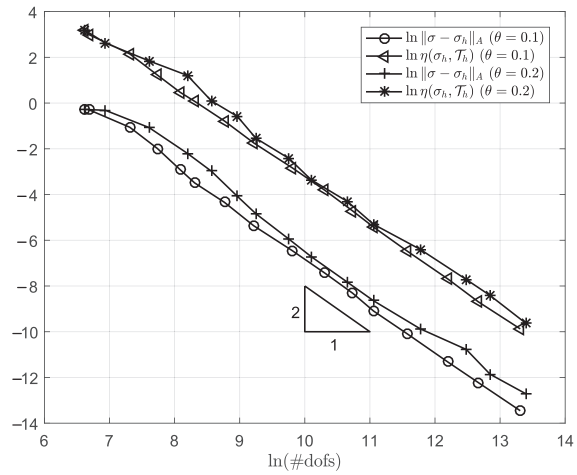

Figure 2 Errors $\|\sigma - \sigma_h\|_A$ and $\eta(\sigma_h, \mathcal{T}_h)$ vs. #dofs in ln-ln scale for Example 2 with $\lambda = 10$

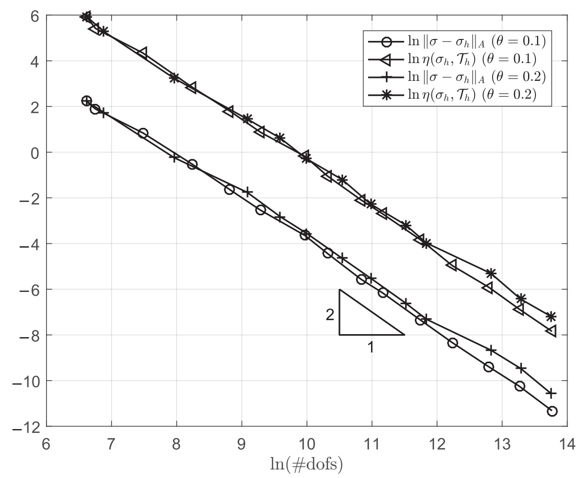

Figure 3 Errors $\|\sigma - \sigma_h\|_A$ and $\eta(\sigma_h, \mathcal{T}_h)$ vs. #dofs in ln-ln scale for Example 2 with $\lambda = 10{,}000$

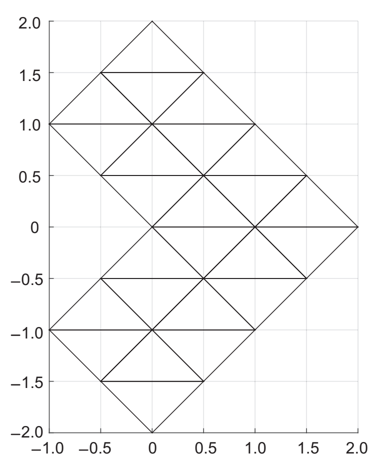

Figure 4 The rotated L-shaped domain with the initial mesh

$\Omega = (-1, 1) \times (-1, 1)\backslash[0, 1) \times (-1, 0]$. Let

$$\Phi_1(\theta) = \begin{pmatrix} \big((z+2)(\lambda+\mu)+4\mu\big)\sin(z\theta) - z(\lambda+\mu)\sin((z-2)\theta) \\ z(\lambda+\mu)\big(\cos(z\theta) - \cos((z-2)\theta)\big) \end{pmatrix},$$

Table 3 Numerical errors for Example 3 with $k = 3$ on uniform meshes

h	$\|\sigma - \sigma_h\|_A$	order	$\eta(\sigma_h, \mathcal{T}_h)$	order	$\eta(\sigma_h, \mathcal{T}_h)/\|\sigma - \sigma_h\|_A$
$\sqrt{2}/2$	6.6585E−03	–	4.5431E−04	–	6.82E−02
$\sqrt{2}/2^2$	4.7264E−03	0.4944	3.2749E−04	0.4722	6.93E−02
$\sqrt{2}/2^3$	3.2966E−03	0.5198	2.3212E−04	0.4966	7.04E−02
$\sqrt{2}/2^4$	2.2791E−03	0.5325	1.6180E−04	0.5207	7.10E−02
$\sqrt{2}/2^5$	1.5689E−03	0.5387	1.1182E−04	0.5330	7.13E−02
$\sqrt{2}/2^6$	1.0777E−03	0.5418	7.6957E−05	0.5390	7.14E−02
$\sqrt{2}/2^7$	7.3957E−04	0.5432	5.2859E−05	0.5419	7.15E−02

Table 4 Numerical errors for Example 3 with $k = 4$ on uniform meshes

h	$\|\sigma - \sigma_h\|_A$	order	$\eta(\sigma_h, \mathcal{T}_h)$	order	$\eta(\sigma_h, \mathcal{T}_h)/\|\sigma - \sigma_h\|_A$
$\sqrt{2}/2$	5.3787E−03	–	8.4604E−04	–	1.57E−01
$\sqrt{2}/2^2$	3.7715E−03	0.5121	6.0103E−04	0.4933	1.59E−01
$\sqrt{2}/2^3$	2.6141E−03	0.5288	4.2105E−04	0.5134	1.61E−01
$\sqrt{2}/2^4$	1.8017E−03	0.5370	2.9171E−04	0.5294	1.62E−01
$\sqrt{2}/2^5$	1.2383E−03	0.5409	2.0101E−04	0.5373	1.62E−01
$\sqrt{2}/2^6$	8.5005E−04	0.5428	1.3814E−04	0.5411	1.63E−01

Table 5 Numerical errors for Example 3 with $k = 5$ on uniform meshes

h	$\|\sigma - \sigma_h\|_A$	order	$\eta(\sigma_h, \mathcal{T}_h)$	order	$\eta(\sigma_h, \mathcal{T}_h)/\|\sigma - \sigma_h\|_A$
$\sqrt{2}/2$	4.5148E−03	–	1.2961E−03	–	2.87E−01
$\sqrt{2}/2^2$	3.1444E−03	0.5219	9.1388E−04	0.5041	2.91E−01
$\sqrt{2}/2^3$	2.1721E−03	0.5337	6.3609E−04	0.5228	2.93E−01
$\sqrt{2}/2^4$	1.4946E−03	0.5393	4.3929E−04	0.5341	2.94E−01
$\sqrt{2}/2^5$	1.0265E−03	0.5420	3.0223E−04	0.5395	2.94E−01

$$\Phi_2(\theta) = \begin{pmatrix} z(\lambda+\mu)(\cos((z-2)\theta) - \cos(z\theta)) \\ -((2-z)(\lambda+\mu)+4\mu)\sin(z\theta) - z(\lambda+\mu)\sin((z-2)\theta) \end{pmatrix},$$
$$\begin{aligned}\Phi(\theta) &= (z(\lambda+\mu)\sin((z-2)\omega) + ((2-z)(\lambda+\mu)+4\mu)\sin(z\omega))\Phi_1(\theta) \\ &\quad - z(\lambda+\mu)(\cos((z-2)\omega) - \cos(z\omega))\Phi_2(\theta),\end{aligned}$$

where $z \in (0,1)$ is a real root of $(\lambda+3\mu)^2\sin^2(z\omega) = (\lambda+\mu)^2 z^2 \sin^2\omega$ with $\omega = 3\pi/2$. The exact singular solution in polar coordinates is taken as (see [24, Subsection 4.6])

$$u(r,\theta) = \frac{1}{(\lambda+\mu)^2}(r^2\cos^2\theta - 1)(r^2\sin^2\theta - 1)r^z\Phi(\theta).$$

It can be computed that $z = 0.561586549334359$ for $\lambda = 10$, and $z = 0.544505718203590$ for $\lambda = 10{,}000$. We also take $k = 3$ and $\mu = 1$.

Some meshes generated by Algorithm 1 for different bulk parameter ϑ and Lamé constant λ are shown in Figure 1, where #dofs is the number of degrees of freedom. The adaptive Algorithm 1 captures the singularity of the exact solution on the corner $(0,0)$ very well. The histories of the adaptive Algorithm 1 for $\vartheta = 0.1, \vartheta = 0.2$ and $\lambda = 10, \lambda = 10{,}000$ are presented in Figures 2 and 3. We can see from Figures 2 and 3 that the convergence rates of errors $\|\sigma - \sigma_h\|_A$ and $\eta(\sigma_h, \mathcal{T}_h)$ are both $O((\#\text{dofs})^{-2})$ no matter $\lambda = 10$ or $\lambda = 10{,}000$, which demonstrates the theoretical results. For uniform grid, $\#(\text{dofs})^{-2} \cong h^4$, this means that the errors $\|\sigma - \sigma_h\|_A$ and $\eta(\sigma_h, \mathcal{T}_h)$ converge with an optimal rate.

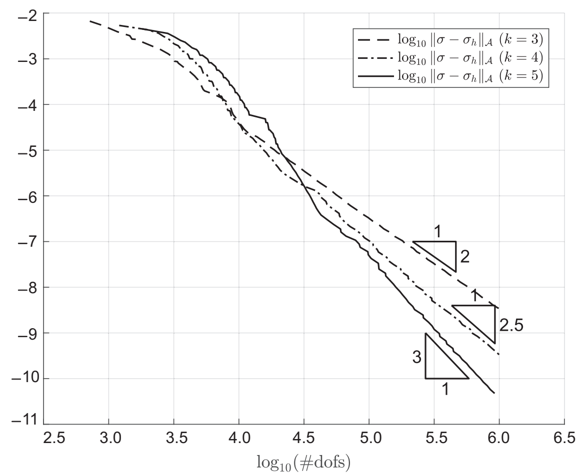

Figure 5 Errors $\|\sigma-\sigma_h\|_A$ vs. #dofs in $\log_{10}$-$\log_{10}$ scale for Example 3 with $\vartheta=0.1$

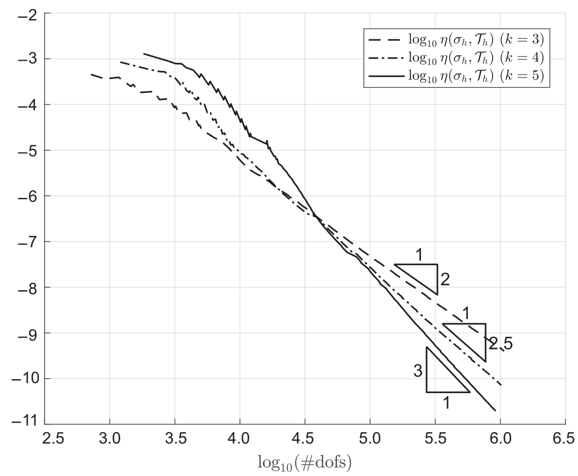

Figure 6 Errors $\eta(\sigma_h,\mathcal{T}_h)$ vs. #dofs in $\log_{10}$-$\log_{10}$ scale for Example 3 with $\vartheta=0.1$

The third example considers the L-shape benchmark problem with general boundary conditions testified in [16, Subsection 5.3] on the rotated L-shaped domain with the initial mesh as depicted in Figure 4. We impose the Neumann boundary condition on the boundary $x^2=y^2$ and the Dirichlet boundary condition on the rest boundary of Ω. The exact solution in the polar coordinates is given as follows:

$$\begin{pmatrix} u_r(r,\theta) \\ u_\theta(r,\theta) \end{pmatrix} = \frac{r^\alpha}{2\mu} \begin{pmatrix} -(\alpha+1)\cos((\alpha+1)\theta)+(C_2-\alpha-1)C_1\cos((\alpha-1)\theta) \\ (\alpha+1)\sin((\alpha+1)\theta)+(C_2+\alpha-1)C_1\sin((\alpha-1)\theta) \end{pmatrix}.$$

The constants are $C_1 := -\cos((\alpha+1)\omega)/\cos((\alpha-1)\omega)$ and $C_2 := -2(\lambda+2\mu)/(\lambda+\mu)$, where $\alpha = 0.544483736782$ is the positive solution of $\alpha\sin(2\omega)+\sin(2\omega\alpha)=0$ for $\omega=3\pi/4$. The Lamé parameters

$$\lambda=\frac{E\nu}{(1+\nu)(1-2\nu)},\quad \mu=\frac{E}{2(1+\nu)}$$

with the elasticity modulus $E=10^5$ and the Poisson ratio $\nu=0.4999$. The volume force $f(x,y)$ and the Neumann boundary data vanish, and the Dirichlet boundary condition is taken from the exact solution. It is easy to check that $u\in H^s(\Omega;\mathbb{R}^2)$ for any $s<1+\alpha$. The numerical errors for $k=3,4,5$ on uniform meshes are listed in Tables 3–5, from which we observe that both the convergence rates of $\|\sigma-\sigma_h\|_A$ and $\eta(\sigma_h,\mathcal{T}_h)$ are almost $O(h^\alpha)$ indicated by the regularity of the exact solution u. Hence adopting higher order finite elements on the uniform meshes does not lead to higher convergence rates, because of the singularity of u.

Then we test the *a posteriori* error estimator $\eta(\sigma_h, \mathcal{T}_h)$ on the adaptive meshes. The histories of Algorithm 1 for $k = 3, 4, 5$ and $\vartheta = 0.1$ are presented in Figures 5 and 6, which mean that the convergence rates of errors $\|\sigma - \sigma_h\|_A$ and $\eta(\sigma_h, \mathcal{T}_h)$ are both optimal, i.e., $O((\#\text{dofs})^{-(k+1)/2})$.

Acknowledgements This work was supported by National Science Foundation of USA (Grant No. DMS-1418934), the Sea Poly Project of Beijing Overseas Talents, National Natural Science Foundation of China (Grant Nos. 11625101, 91430213, 11421101, 11771338, 11671304 and 11401026), Zhejiang Provincial Natural Science Foundation of China Projects (Grant Nos. LY17A010010, LY15A010015 and LY15A010016) and Wenzhou Science and Technology Plan Project (Grant No. G20160019). The last author thanks the support of the China Scholarship Council and the University of California, Irvine during her visit to UC Irvine from 2014 to 2015.

References

1 Adams S, Cockburn B. A mixed finite element method for elasticity in three dimensions. J Sci Comput, 2001, 25: 515–521

2 Alonso A. Error estimators for a mixed method. Numer Math, 1996, 74: 385–395

3 Arnold D N. Differential complexes and numerical stability. In: Proceedings of the International Congress of Mathematicians, vol 1. Beijing: Higher Education Press, 2002, 137–157

4 Arnold D N, Awanou G. Rectangular mixed finite elements for elasticity. Math Models Methods Appl Sci, 2005, 15: 1417–1429

5 Arnold D N, Awanou G, Winther R. Finite elements for symmetric tensors in three dimensions. Math Comp, 2008, 77: 1229–1251

6 Arnold D N, Brezzi F, Douglas J. Peers: A new mixed finite element for plane elasticity. Jpn J Appl Math, 1984, 1: 347–367

7 Arnold D N, Falk R S, Winther R. Mixed finite element methods for linear elasticity with weakly imposed symmetry. Math Comp, 2007, 76: 1699–1724

8 Arnold D N, Winther R. Mixed finite elements for elasticity. Numer Math, 2002, 92: 401–419

9 Arnold D N, Winther R. Nonconforming mixed elements for elasticity. Math Models Methods Appl Sci, 2003, 13: 295–307

10 Boffi D, Brezzi F, Fortin M. Reduced symmetry elements in linear elasticity. Commun Pure Appl Anal, 2009, 8: 95–121

11 Boffi D, Brezzi F, Fortin M. Mixed Finite Element Methods and Applications. Springer Series in Computational Mathematics, vol. 44. Heidelberg: Springer, 2013

12 Bramble J H, Xu J. A local post-processing technique for improving the accuracy in mixed finite-element approximations. SIAM J Numer Anal, 1989, 26: 1267–1275

13 Carstensen C. A posteriori error estimate for the mixed finite element method. Math Comp, 1997, 66: 465–477

14 Carstensen C, Dolzmann G. A posteriori error estimates for mixed FEM in elasticity. Numer Math, 1998, 81: 187–209

15 Carstensen C, Eigel M, Gedicke J. Computational competition of symmetric mixed FEM in linear elasticity. Comput Methods Appl Mech Engrg, 2011, 200: 2903–2915

16 Carstensen C, Gedicke J. Robust residual-based a posteriori Arnold-Winther mixed finite element analysis in elasticity. Comput Methods Appl Mech Engrg, 2016, 300: 245–264

17 Carstensen C, Günther D, Reininghaus J, et al. The Arnold-Winther mixed FEM in linear elasticity. Part I: Implementation and numerical verification. Comput Methods Appl Mech Engrg, 2008, 197: 3014–3023

18 Carstensen C, Hu J. A unifying theory of a posteriori error control for nonconforming finite element methods. Numer Math, 2007, 107: 473–502

19 Chen L, Holst M, Xu J. Convergence and optimality of adaptive mixed finite element methods. Math Comp, 2009, 78: 35–35

20 Chen L, Hu J, Huang X. Fast auxiliary space preconditioner for linear elasticity in mixed form. Math Comp, 2017, https://doi.org/10.1090/mcom/3285

21 Cockburn B, Gopalakrishnan J, Guzmán J. A new elasticity element made for enforcing weak stress symmetry. Math Comp, 2010, 79: 1331–1349

22 Gatica G N, Maischak M. A posteriori error estimates for the mixed finite element method with Lagrange multipliers. Numer Methods Partial Differential Equations, 2005, 21: 421–450

23 Girault V, Scott L R. Hermite interpolation of nonsmooth functions preserving boundary conditions. Math Comp, 2002, 71: 1043–1074

24 Grisvard P. Singularities in Boundary Value Problems. Research in Applied Mathematics, vol. 22. Paris: Masson, 1992

25 Guzmán J. A unified analysis of several mixed methods for elasticity with weak stress symmetry. J Sci Comput, 2010, 44: 156–169
26 Hoppe R H W, Wohlmuth B. Adaptive multilevel techniques for mixed finite element discretizations of elliptic boundary value problems. SIAM J Numer Anal, 1997, 34: 1658–1681
27 Hu J. Finite element approximations of symmetric tensors on simplicial grids in $\mathbb{R}^n$: The higher order case. J Comput Math, 2015, 33: 283–296
28 Hu J. A new family of efficient conforming mixed finite elements on both rectangular and cuboid meshes for linear elasticity in the symmetric formulation. SIAM J Numer Anal, 2015, 53: 1438–1463
29 Hu J, Zhang S. A family of conforming mixed finite elements for linear elasticity on triangular grids. ArXiv:1406.7457, 2014
30 Hu J, Zhang S. A family of symmetric mixed finite elements for linear elasticity on tetrahedral grids. Sci China Math, 2015, 58: 297–307
31 Hu J, Zhang S. Finite element approximations of symmetric tensors on simplicial grids in $\mathbb{R}^n$: The lower order case. Math Models Methods Appl Sci, 2016, 26: 1649–1669
32 Kim K Y. A posteriori error estimator for linear elasticity based on nonsymmetric stress tensor approximation. J Korean Soc Ind Appl Math, 2012, 16: 1–13
33 Larson M G, Målqvist A. A posteriori error estimates for mixed finite element approximations of elliptic problems. Numer Math, 2008, 108: 487–500
34 Lonsing M, Verfürth R. A posteriori error estimators for mixed finite element methods in linear elasticity. Numer Math, 2004, 97: 757–778
35 Lovadina C, Stenberg R. Energy norm a posteriori error estimates for mixed finite element methods. Math Comp, 2006, 75: 1659–1674
36 Morgan J, Scott R. A nodal basis for C^1 piecewise polynomials of degree $n \geqslant 5$. Math Comp, 1975, 29: 736–740
37 Shi Z C, Wang M. Finite Element Methods. Beijing: Science Press, 2013
38 Stenberg R. A family of mixed finite elements for the elasticity problem. Numer Math, 1988, 53: 513–538